

NRL REPORT 3823

**RELATIVE RADIATION DENSITY AND TEMPERATURE
DISTRIBUTION OF ROCKET FLAMES**



**APPROVED FOR PUBLIC
RELEASE - DISTRIBUTION
UNLIMITED**

**NAVAL RESEARCH LABORATORY
WASHINGTON, D.C.**



**RELATIVE RADIATION DENSITY AND TEMPERATURE
DISTRIBUTION OF ROCKET FLAMES**

F. E. Wyman

July 10, 1951

Approved by:

F. M. Gager, Head, Special Research Branch
R. M. Page, Superintendent, Radio Division III

NAVAL RESEARCH LABORATORY

CAPTAIN F. R. FURTH, USN, DIRECTOR
WASHINGTON, D.C.



DISTRIBUTION

OpNav	
Attn: Op-42	2
ONR	
Attn: Code 470	1
CDR, NATC	
Attn: Electronics Test	1
Wright-Patterson AFB	
Attn: BAU-CADO	1
Attn: CADO-E1	2
Attn: Ch., Electronics Subdiv., MCREEO-2	1
CO, AMC, Watson Labs., Red Bank	
Attn: ENR	1
CO, Air Force Cambridge Res. Labs.	
Attn: ERRS	1
CG, SCEL	
Attn: SCEL Liaison Office	3
Dir., NBS	
Attn: CRPL	1
Attn: Dr. W. S. Benedict	1
Attn: Dr. E.K. Plyler	1
RDB	
Attn: Information Requirements Branch	2
Attn: Navy Secretary	1
ANAF/GM Mailing List No. 14, Parts A, C, DG, & DP	

CONTENTS

Abstract	iv
Problem Status	iv
Authorization	iv
INTRODUCTION	1
METHOD OF INVESTIGATION	2
RESULTS	8
Physical Dimensions	8
Node Position	9
Radiation Density	10
Temperature Distribution	10
SUMMARY	19
FUTURE PLANS	19
ACKNOWLEDGMENT	19

ABSTRACT

This report discusses a method of determining relative radiation density and temperature distribution of rocket exhaust flames by photographic methods. Total radiant-energy data is obtained from a photographic negative and, by graphical differentiation and integration, is converted to relative radiation density. Temperature distribution is calculated upon the basis of an assumed temperature at a known position in the flame. Flame dimensions and node positions of several motor runs are presented for completeness.

PROBLEM STATUS

This is an interim report on the problem; work is continuing.

AUTHORIZATION

*NRL Problem R11-13R
NR 511-130*

Manuscript submitted for publication: March 21, 1951

RELATIVE RADIATION DENSITY AND TEMPERATURE DISTRIBUTION OF ROCKET FLAMES

INTRODUCTION

The investigation of the physical properties of rocket exhaust flames has been of considerable interest in recent years. This interest stems from several lines of work. The advent of rockets as military weapons has occasioned considerable design work in the field of reaction motors. A reasonably satisfactory design theory has been developed, and from the academic standpoint many of the problems in this field have been passed over. The necessity to reduce some aspects of the theory to practice reopened numerous questions.

The gases in the exhaust flame of the rockets under consideration are traveling with supersonic velocities, and any disturbance occurring in the flame passes down the flame faster than it can be propagated up stream to the motor. For this reason it would seem that physical properties of the flame would be of little interest. Nevertheless a measurement of the condition within the combustion chamber, along with the geometric factors of the chamber and expansion throat, allow, with assumptions, theoretical calculation of certain properties of the gases in the flame. An agreement between calculated and experimentally measured values would give confidence in the theory.

The problem of designing rocket motors also renewed interest in the principles of combustion. Here again the flame, after it has left the combustion chamber, became a point of interest. It was realized that under certain expansion conditions some combustion continued after the gas had exhausted from the motor.

Finally, the problem of rocket guidance pointed to a necessity for knowledge of the electromagnetic properties of the flame and its trail. In those rockets where all guidance intelligence arrives in the form of electromagnetic energy, and in the particular case of a beam-riding rocket, much of the electromagnetic energy may be required to pass through the exhaust gases. The quasi-optical properties thus become important, and this immediately brings up the question of the nature and degree of attenuation of the electromagnetic signal one might expect.

In all three of these fields an important physical property of the flame is the temperature. Unfortunately, because of the supersonic velocities encountered in a rocket flame, direct measurements of temperature by obvious methods are impossible. Any probe or measuring instrument that might be inserted into the flame would rapidly erode away or be melted by the high temperature. Even if this were not so, the probe would so alter the flow of gases that indicated temperature would not be the true temperature of the undisturbed flame at the chosen point of probe insertion. For this reason methods of measuring temperature depending upon the radiation in the visible or near-visible region of the spectrum appear to be the most promising.

Existing theory is adequate for such radiation measurements, but the problem of adequate instrumentation presents many serious difficulties. In the first place, the acoustic fields near the rocket flame contain very-high-level sound pressure variations of somewhat random frequency distribution. This condition alone presents the difficult problem of operating precision optical

NAVAL RESEARCH LABORATORY

instruments in close proximity to rocket flames, and, in addition, the ever-present danger of explosion and the acute discomfort to human beings working near the rocket necessitates remote operation of any measuring equipment.

A further instrumentation difficulty to be overcome is the comparatively low level of radiation emanating from the rocket flame and the short firing duration of a rocket motor. These latter factors call for highly sensitive detectors in spite of their high sensitivity to mechanical vibration. Together these instrumentation difficulties constitute a situation that has not been satisfactorily solved.

The work with which this report is concerned has been limited in the main to the determination of relative temperature distribution for two specific rocket motors; the 400-lb-thrust acid-aniline and the 1500-lb-thrust oxygen-alcohol motors manufactured by Reaction Motors, Inc. of Rockway, New Jersey. These motors were examined at sea level under static-thrust conditions, and the data presented subsequently shows temperature at selected regions in the flame after suitable assumption has been made as to the temperature at a given point. Probably the most important accomplishment is the demonstration that a rocket flame in static thrust is anything but a homogenous temperature barrier. In fact it confirms, beyond doubt, the suspicion that a rocket flame is a very complex barrier, so much so, as to tend to discourage detailed investigation. The latter is of value in that it may discourage expression of attenuation data in terms of decibels per meter, since a homogenous region approaching a meter in length is not to be found.

The data presented subsequently as a result of specific investigations can be grouped as follows:

- (a) Physical dimensions of flame
- (b) Position of Mach nodes
- (c) Distribution of radiation density
- (d) Distribution of temperature based upon specific assumption.

METHOD OF INVESTIGATION

The method used in this investigation was suggested by a German report¹ which presents a photographic method of determination of relative radiation density, temperature distribution, and physical dimensions. Negatives are exposed in the test cells and densities measured in the Laboratory. By means of graphical differentiation and integration, radiation density and temperature is calculated.

A 4" x 5" Speed Graphic camera equipped with standard Navy optics was placed on a heavy tripod to one side of the flame in such a manner that the camera axis met the axis of the flame at right angles at a point approximately midway down the flame (Figure 1). The distance from the lens to the flame axis was adjusted so that the image of the flame filled most of the usable length of the negative. The image-reduction ratio was determined by placing three small incandescent lamps at known points in the position of the flame and photographing them with the standard camera setup. By comparing the image distance between the lamps with their

¹ Frieser, H., "Optical and Photographic Investigation of the Flame," Germany Archiv Nr. 38/lgk, translated by General Electric Company, Data Folder 85514 (Restricted), March 1947

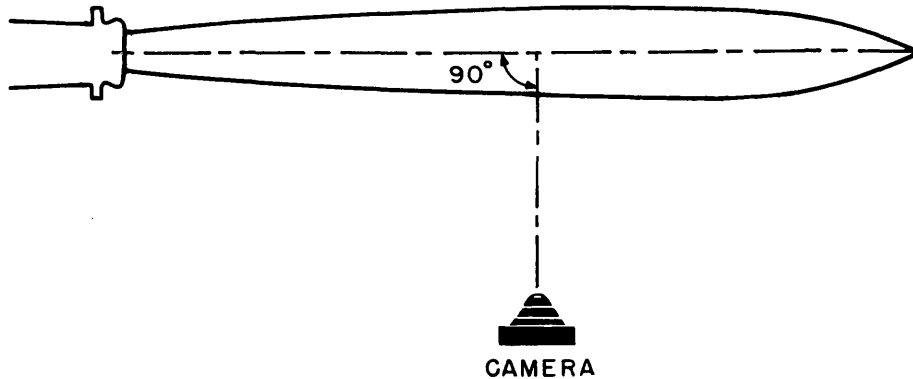


Figure 1 - Position of camera relative to flame

actual distances, the reduction ratio was calculated. It was determined that distortion of distances measured at the edge of the plate was less than the over-all accuracy desired and hence their distortion was neglected.

Two types of photographic negative material were used. For the exposures using infrared radiation, Eastman Kodak infrared sheet film was used in conjunction with a No. 87 Wratten filter. For the visible-light exposure, Eastman Kodak Portrait Panchromatic cut film was used without a filter. The transmission band of the infrared film-filter combination was about 7400 A to 8550 A, as shown in Figure 2, and the transmission band for the exposures made by visible light was that of Eastman type B panchromatic film.

The camera was loaded before the rocket motor was fired and the exposure made by remote release after stable motor operating conditions had been established. Immediately after the run a previously shielded and unexposed portion of the film was exposed through the appropriate filter and a calibrated step wedge of graduated neutral densities. All film was processed on location to be sure that suitable and sufficient exposures were obtained.

On arrival at the Naval Research Laboratory, the negatives were analyzed by means of a Leeds and Northrup recording microdensitometer. The negatives were traversed along the axis of the flame image to determine the flame length and the position of the Mach nodes. Other traverses were made across the flame image at right angles to the axis at selected points, as shown in Figure 3. Typical recorder traces from the microdensitometer are shown in Figure 4.

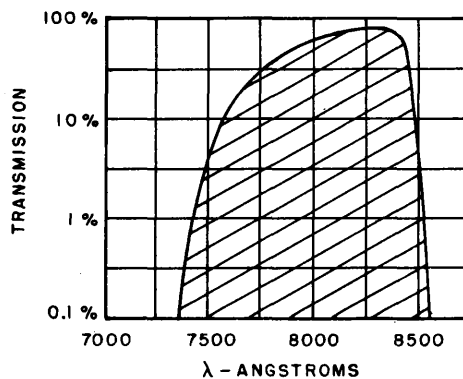


Figure 2 - Transmission of infrared plate with Wratten No. 87 filter

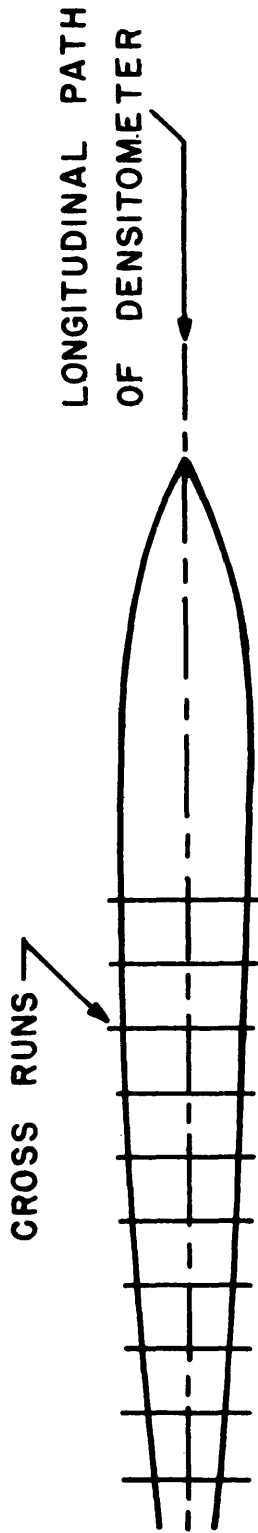


Figure 3 - Typical densitometer traverses

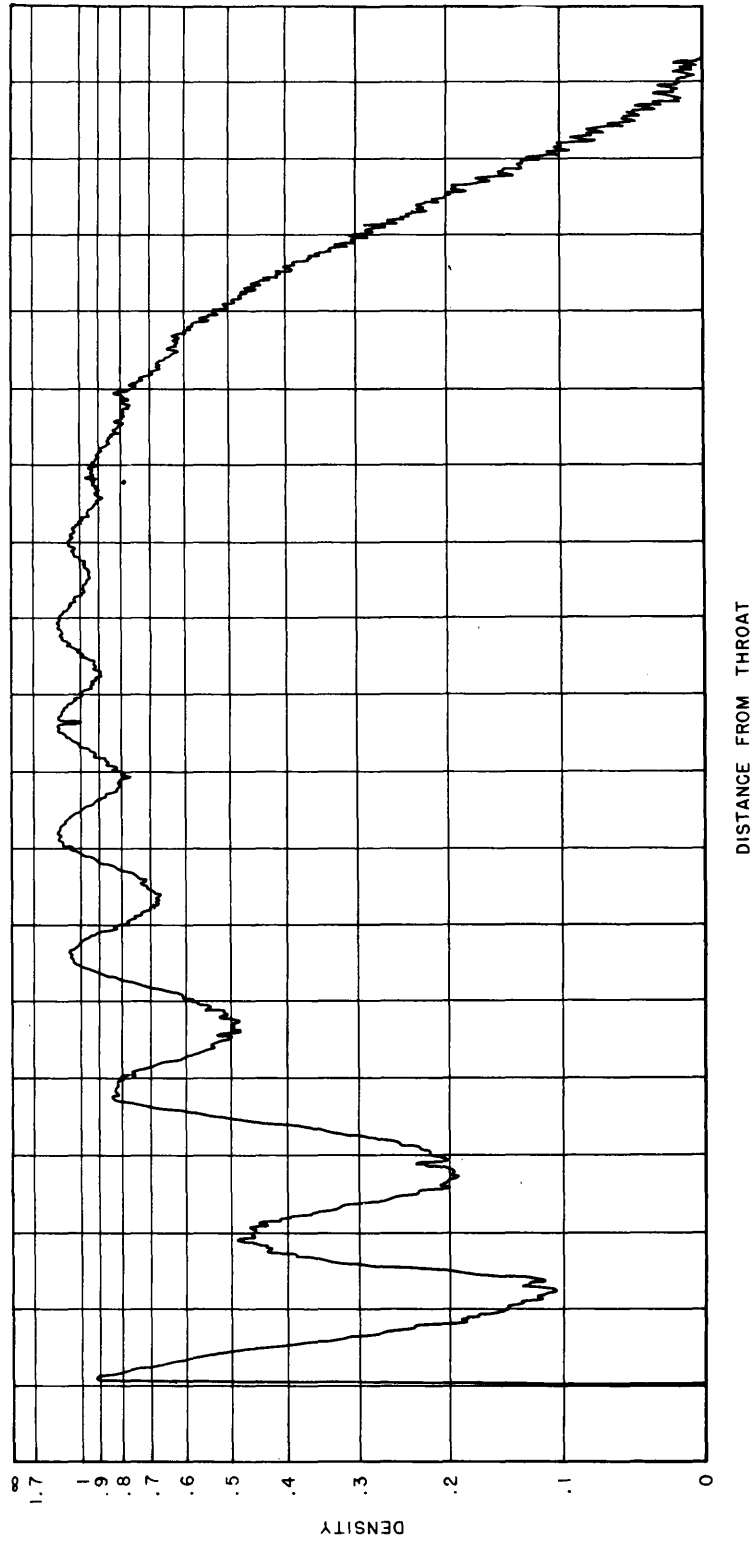


Figure 4 - Typical densitometer trace along longitudinal axis of flame

From recordings of this type optical density can be tabulated as a function of position. Along the side of each negative is the print of a step wedge. Since densities of the master wedge from which each was printed are known, the relative exposure that produced each step on the negative is also known. It is then possible to plot relative exposure against density and have a calibration of the particular negative under consideration. The radiant energy producing a particular density is directly proportional to the relative exposure, and curves of relative radiant energy versus position on a cross run can be plotted.

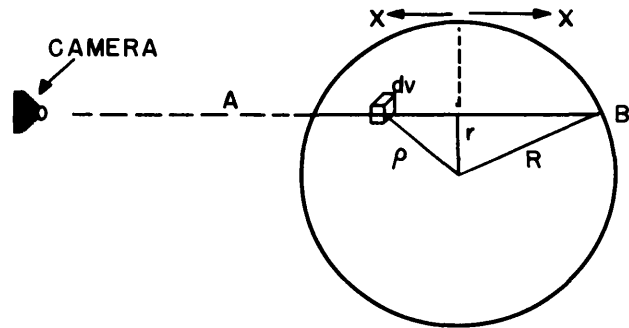


Figure 5

The total relative radiant energy, U , as experimentally determined, is the result of all radiant energy emanating along line AB of Figure 5. A more useful quantity is radiation density:

$$u = \frac{dU}{dV} .$$

The experimentally determined radiant energy is a function of the vertical distance, r ; it can be written:

$$U(r) = 2 \int_{x=0}^{x=\sqrt{R^2 - r^2}} u(\rho) dx \quad (1)$$

if rotational symmetry is assumed. Accomplishing a change in variable, Equation (1) can be written:

$$U(r) = 2 \int_{\rho=r}^{\rho=R} \frac{u(\rho) \rho d\rho}{\sqrt{\rho^2 - r^2}} . \quad (2)$$

This integral equation has been solved² to give:

$$u(\rho) = -\frac{1}{\pi} \int_{r=\rho}^{r=R} \frac{dU(r)}{dr} \frac{dr}{\sqrt{r^2 - \rho^2}} . \quad (3)$$

The complexity of the solution of Equation (3) forces one to graphical evaluation. Owing to the singularity at $r = \rho$, a substitution is helpful.

² Frieser, *op. cit.*

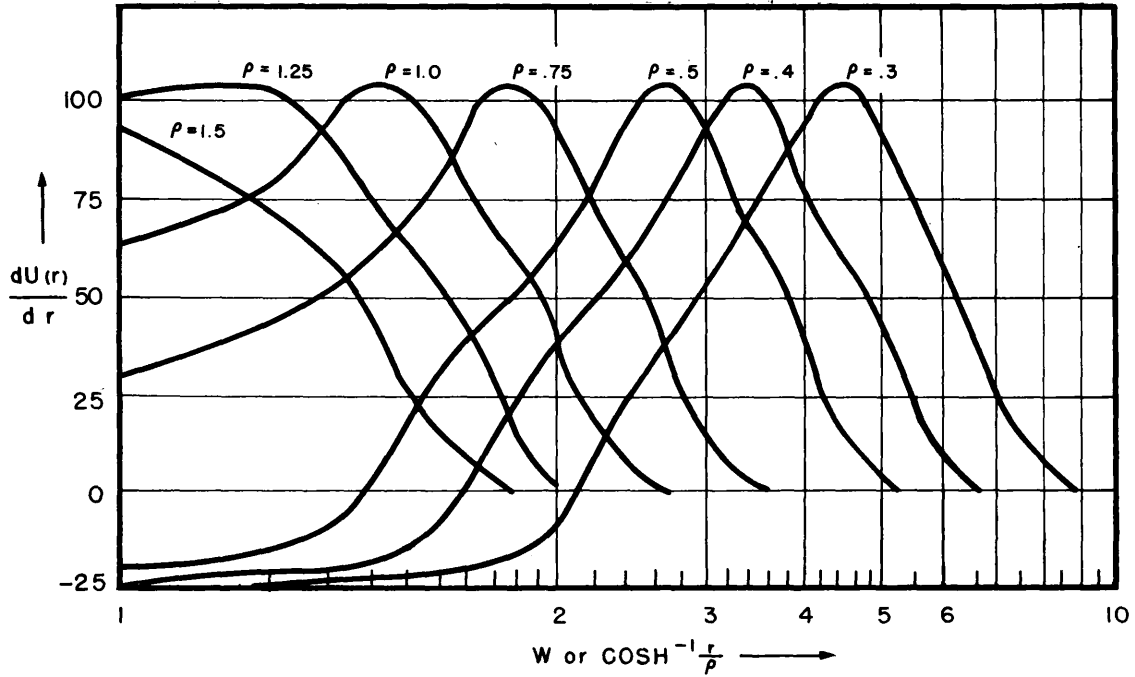


Figure 6

Let

$$\cosh^{-1} r/\rho = w$$

$$\cosh w = r/\rho$$

$$\sinh w dw = dr/\rho$$

$$dw = dr/\rho \sinh w$$

$$\text{but } \sinh w = \sqrt{\frac{r^2}{\rho^2} - 1} .$$

Substituting in Equation (3) and changing variable of integration,

$$u(\rho) = -\frac{1}{\pi} \int_{w=0}^{w = \cosh^{-1} R/\rho} \frac{dU[r(w)]}{dr} dw \quad (4)$$

The density data, $U(r)$, is given for each value of r . Theory assumes symmetry about the flame axis, and for further calculation only one of the symmetrical half curves is used. The experimental curves lack symmetry to a small degree, and for this reason a composite curve, being the average of the two, was prepared and differentiated graphically. The values of $dU(r)/dr$ resulting from this differentiation are placed upon a specially prepared coordinate grid the abscissa of which is ruled in $\cosh^{-1} r/\rho$, i.e., w . By planimetering the area bounded by the curve and the abscissa, $u(\rho)$ is determined for one value of ρ except for a constant factor. Hence relative radiation density is determined. A typical example of such a plot is shown in Figure 6.

The results of these calculations give information of considerable interest, but further calculation allows conversion to relative temperature according to Wein's law,

$$u = \frac{c_1}{\lambda^5} e^{-c_2/\lambda T} \cdot \alpha \quad (5)$$

where α is the absorption coefficient and λ is the wavelength in use. Let the relative radiation density $u = k u'$, where k is constant and u' is the absolute radiation density. Then

$$u_1 = \frac{c_1}{\lambda^5} e^{-c_2/\lambda T_1} \cdot \alpha$$

$$\log u_1 - \log \frac{c_1}{\lambda^5} - \log \alpha = - \frac{.43 c_2}{\lambda} \cdot \frac{1}{T_1}$$

or

$$\log u_1 + K = - \frac{.43 c_2}{\lambda} \cdot \frac{1}{T_1}$$

For a second point in the flame,

$$\log u_2 + K = - \frac{.43 c_2}{\lambda} \cdot \frac{1}{T_2}$$

Subtracting,

$$\log u_1 - \log u_2 = - \frac{.43 c_2}{\lambda} \left(\frac{1}{T_1} - \frac{1}{T_2} \right)$$

or

$$\Delta \log u = - \frac{.43 c_2}{\lambda} \Delta \frac{1}{T} \quad (6)$$

If the temperature is known at one of the points for which the relative radiation density is known, the temperature can be calculated for all other points for which the radiation density is known. Unfortunately, a temperature distribution must be given in terms of a measured or assumed temperature. Owing to the nature of Equation (6), the distribution will change with different values of T .

TABLE 1

Motor Run No.	Motor	Stop	Shutter	Filter	Time of Day	Film	Pressure
13	400 lbs Acid-aniline	f 22	1/200 sec	No. 87	Night	Infrared	450 lbs Standard
16	400 lbs Acid-aniline	f 16	1/200 sec	None	Night	Portrait Pan	450 lbs Standard
28	1500 lbs Oxygen-alcohol	f 12.5	1/50 sec	None	Night	Portrait Pan	228 lbs Chamber 300 lbs Inlet Standard
38	1500 lbs Oxygen-alcohol	f 12.5	1/10 sec	No. 87	Night	Infrared	228 lbs Chamber 300 lbs Inlet Standard
39	1500 lbs Oxygen-alcohol	f 12.5	1/10 sec	No. 87	Night	Infrared	194 lbs Chamber 249 lbs Inlet Below Standard

RESULTS

Forty-four photographic negatives were exposed in the course of a field trip. Of this number, some were consumed in determining the exposure for the flame image and the calibration step wedge. Still others were used for image-ratio calibration. Of those remaining, a group was considered satisfactory for analysis. In view of the very great amount of work involved in this type of analysis, five negatives were chosen for partial or complete analysis. They are negatives number 13, 16, 28, 38, and 39, and the data associated with each of these negatives is given in Table 1. Each negative is a picture of the particular motor run bearing the same number.

Physical Dimensions

Figure 7 shows the actual physical dimensions of the flame as seen by the photographic negative. Experience of subjective nature has shown that there will be slight variations between two successive so-called normal runs. Even though the motor fuel and oxidizer pressures are set by the motor operator, for nominally the same values, the flame will build up to equilibrium conditions in different manners and at different rates. Many of the motor runs used in these experiments were from twenty to thirty seconds duration. While the photographic exposures were made after the flame was judged to have reached equilibrium, undoubtedly some variation is due to different stages of flame growth. Other variations especially those of flame length, can be accounted for by difference in photographic exposures. Along a diameter of the flame the temperature

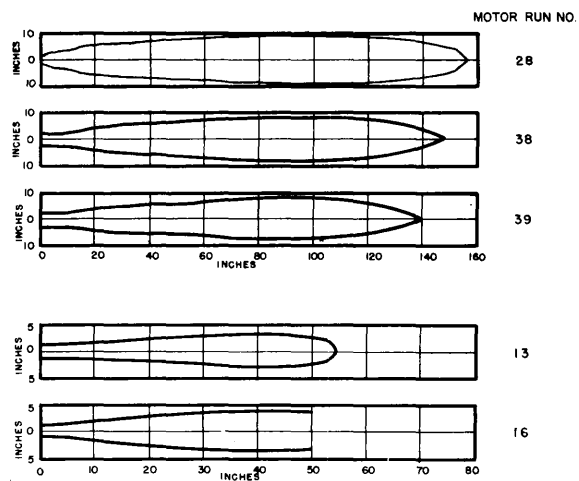


Figure 7 - Actual flame dimensions

TABLE 2

Motor Run No.	Distance of Node from Throat, Inches											Conditions
	1	2	3	4	5	6	7	8	9	10	11	
13	5.5	11.6	17.1	21.4	26.0	29.9	33.6	36.6				Acid-aniline Infrared radiation Pressure 450 lbs
16	5.4	11.5	16.6	21.5	26.9	29.9	33.2	36.7	39.8	41.7		Acid-aniline Visible radiation Pressure 450 lbs
28	10.1	23.2	34.3	44.9	54.5	62.7	69.9	77.0	83.2			Oxygen-alcohol Visible radiation 228 lbs Chamber 300 lbs Inlet pressure
38	8.7	21.9	32.6	42.8	51.6	59.6	67.2	74.2	80.7	85.7		Oxygen-alcohol Infrared radiation 228 lbs Chamber 300 lbs Inlet pressure
39	8.7	19.7	29.9	39.0	47.6	55.7	62.8	69.4	74.4	80.3	84.6	Oxygen-alcohol Infrared radiation 194 lbs Chamber 249 lbs Inlet pressure

gradient is extremely sharp, and the distance from incandescence temperature to ambient temperature is a matter of one or two inches. Difference in exposure would therefore give very little difference in the width of the image. The temperature gradient is considerably less at the tip of the flame and by similar reasoning would give greater variation in flame length. The problem of flame dimension is always open to discussion, depending upon the accepted definition of the flame boundary. For the purposes of this work, the only region of real interest is the region of temperature high enough to be a possible region of ionization. This region is sure to be less than the region recorded on the negatives, as plotted in Figure 7.

Node Position

Information concerning the position of the Mach nodes is readily available from the analysis of the plates. While this information is of secondary interest in connection with this problem, it is presented here in the interest of completeness. No attempt is made to explain the results shown in Tables 2 and 3 other than to state that some variation could be due to incomplete growth of the flame and to small variations in operating conditions, as discussed in the previous section.

TABLE 3

Motor Run No.	Distance between Nodes, Inches										Radiation	Pressure PSI	
	0-1	1-2	2-3	3-4	4-5	5-6	6-7	7-8	8-9	9-10			
13	5.5	6.1	5.5	4.3	4.6	3.9	3.7	3.0			Infrared	450 lbs	
16	5.4	6.1	5.1	4.9	4.4	4.0	3.3	3.5	3.1	1.9	Visible	450 lbs	
28	10.1	13.1	11.1	10.6	9.6	8.2	7.2	7.1	6.2		Visible	228 lbs Chamber 300 lbs Inlet	
38	8.7	13.2	10.7	10.2	8.8	8.0	7.6	7.0	6.5	5.0	Infrared	228 lbs Chamber 300 lbs Inlet	
39	8.7	11.0	10.2	9.1	8.6	8.1	7.1	6.6	5.0	5.9	4.6	Infrared	194 lbs Chamber 249 lbs Inlet

Radiation Density

Figures 8, 9, 10, and 11 show composite plots of the relative radiation density versus distance from the center of the flame. Small solid curves are placed on the figures in such a way as to show their relative position in the flame. Each curve is positioned in its proper place along the appropriate flame picture and in the proper position with respect to a densitometer trace taken down the flame axis. Each curve represents the radiation density versus distance taken at right angles to the longitudinal axis of the flame.

Certain features of the figures are worth comment. In general, radiation density is greater at a Mach node than at an anti-node. The radiation density increases with each successive Mach node, numbered from the throat, to approximately the fourth node, where it reaches a maximum. The radiation density of further Mach nodes decreases slowly, and the node structure becomes indistinct. It is obvious from the various curves that the point of maximum radiation density is not always on the axis of the flame. This seems reasonable from inspection of the negative images and, to a lesser degree, from the prints from these negatives. Occurrence of multiple peaked curves is without a readily determined order, and no definite explanation of this phenomena is attempted. Nevertheless, some comments are possible. In general, these rocket motors were operated under fuel-rich conditions. Consequently, the hot gases of the vaporized fuel are not completely oxidized when they are expelled from the motor throat. Upon entering the relatively low pressure of the outside atmosphere, the gases overexpand and subsequently contract setting up the first node upon which the occurrence of all others depends. At regions where the partially oxidized gas comes in contact with the atmospheric oxygen, further burning takes place to produce a cylindrical burning region of high radiation density enclosing the main body of gas. Furthermore, as the expanding gases are turned back into the flame, oxygen is apparently carried with them. It is clear that, at regions in the front of a node, the radiation density is greater, as though burning were taking place. A varying cylindrical striation of the flame is indicated. Accordingly, cross sections at right angles to the axis depend only upon the striated structure at the particular point concerned.

Temperature Distribution

Conversion of relative radiation density to temperature requires knowledge of the temperature of the flame at a given point and of the relative radiation density at that point. In addition, the wavelength of the light used in making the exposure must be known, and the light must be confined to a relatively small band. The mean value of the wavelength interval was taken to be 8200 Å (Figure 2) for Run Numbers 13, 38, and 39 (Figures 8, 10, and 11). Run Number 16 (Figure 9) was taken with visible light and therefore does not meet the requirement of a narrow-wavelength interval. The choice of known temperatures was limited to the only readily available figures for comparable types of motors. The known temperature in the case of Run Number 13 (Figure 8, acid-aniline motor) was taken to be 2700°K^3 at the maximum of the fourth Mach node, while in the case of Run Numbers 38 and 39 (Figures 10 and 11, oxygen-alcohol motor) the known value was taken to be 2600°K^4 at the first Mach node. Since these values are likely to be in error for the particular motors and runs, care should be exercised in interpreting the absolute

³ Curcio, J. S., and Butler, C. P., "Optical Radiation from Acid-Aniline Jet Flames," NRL Report N-3097, April 1947

⁴ Bundy, F. P., Johnson, R. H., and Strong, M. H., "Final Report on Optical Studies of Rocket Flame at Malta Test Station," General Electric Project Hermes, Report R50A0506 (Unclassified), June 1950

RELATIVE RADIATION DENSITY



INCHES FROM THROAT

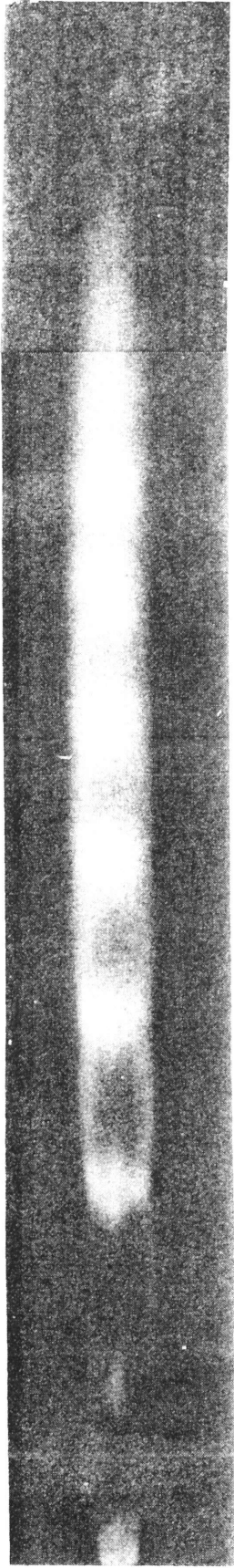
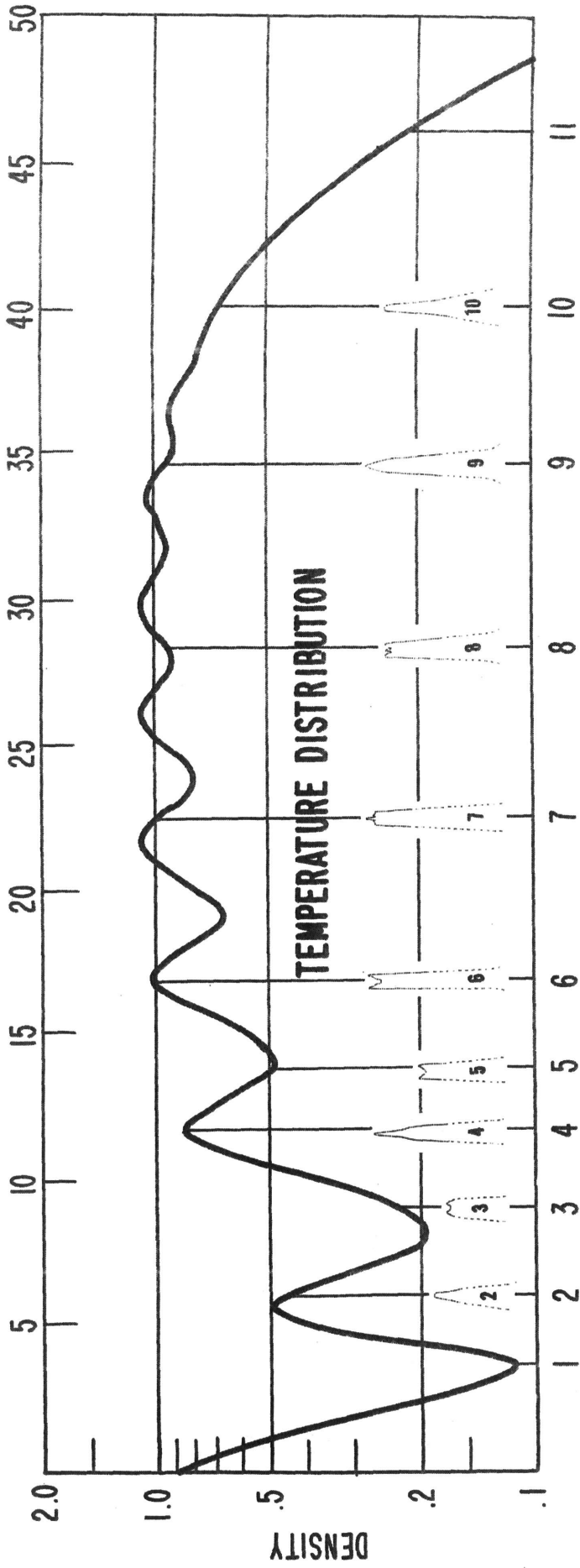


Figure 8 - Motor Run No. 13

This page intentionally left blank.

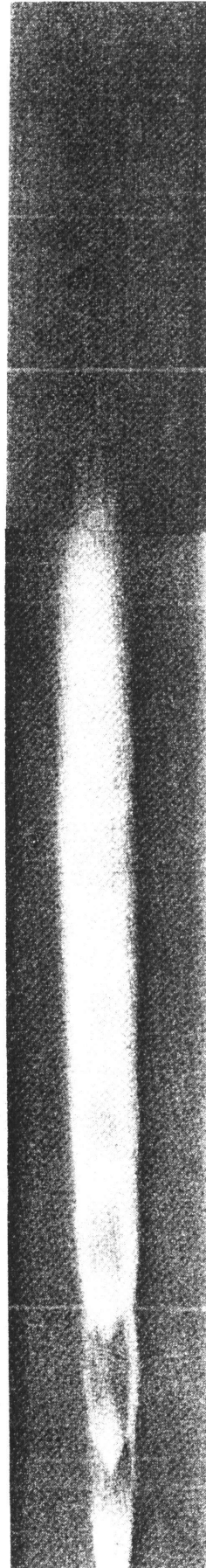
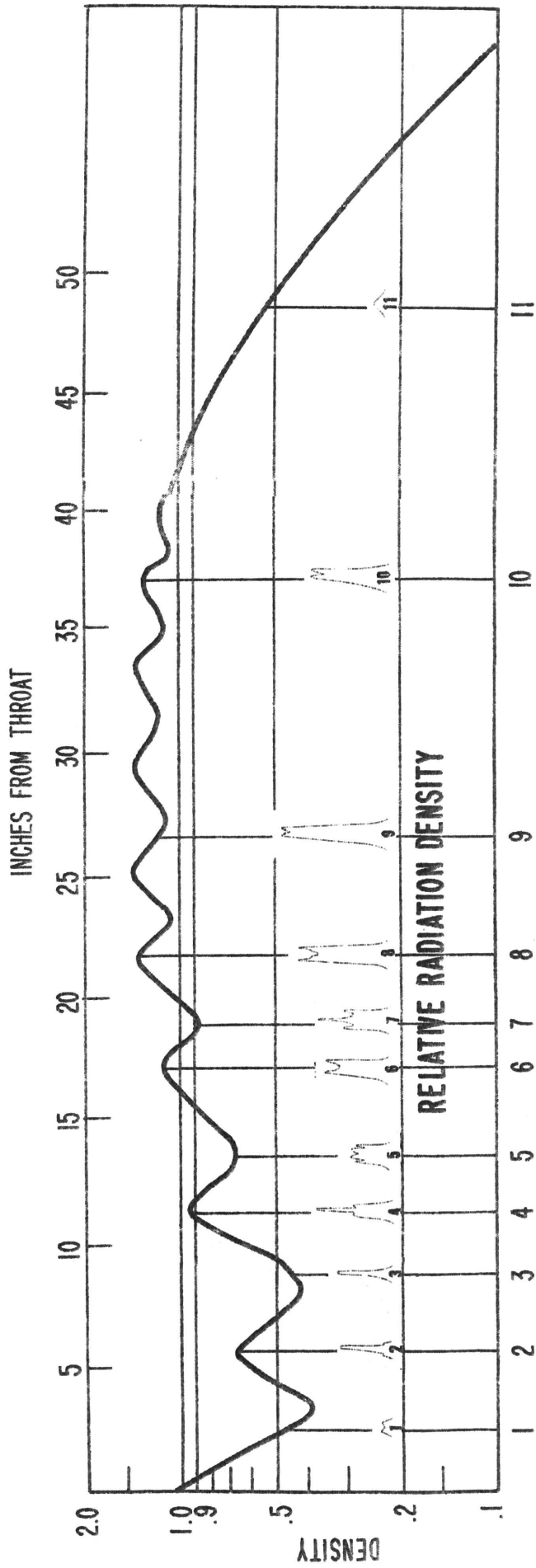
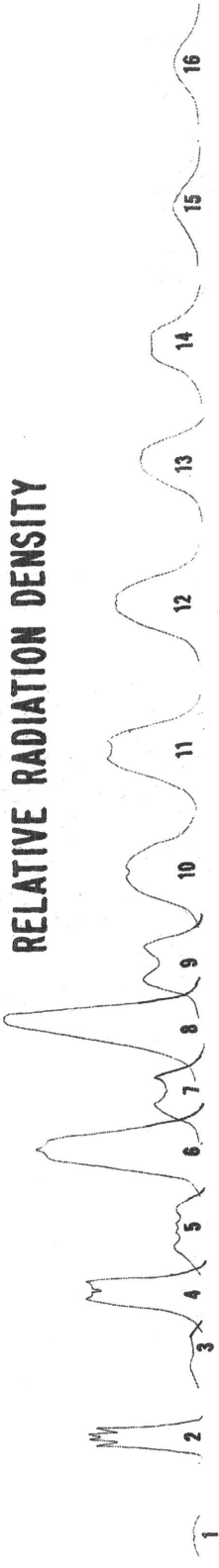


Figure 9 - Motor Run No. 16

This page intentionally left blank.

RELATIVE RADIATION DENSITY



TEMPERATURE DISTRIBUTION

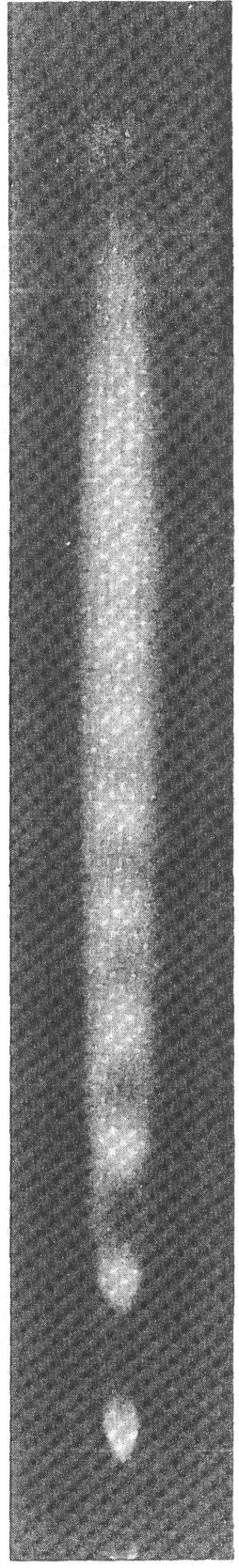
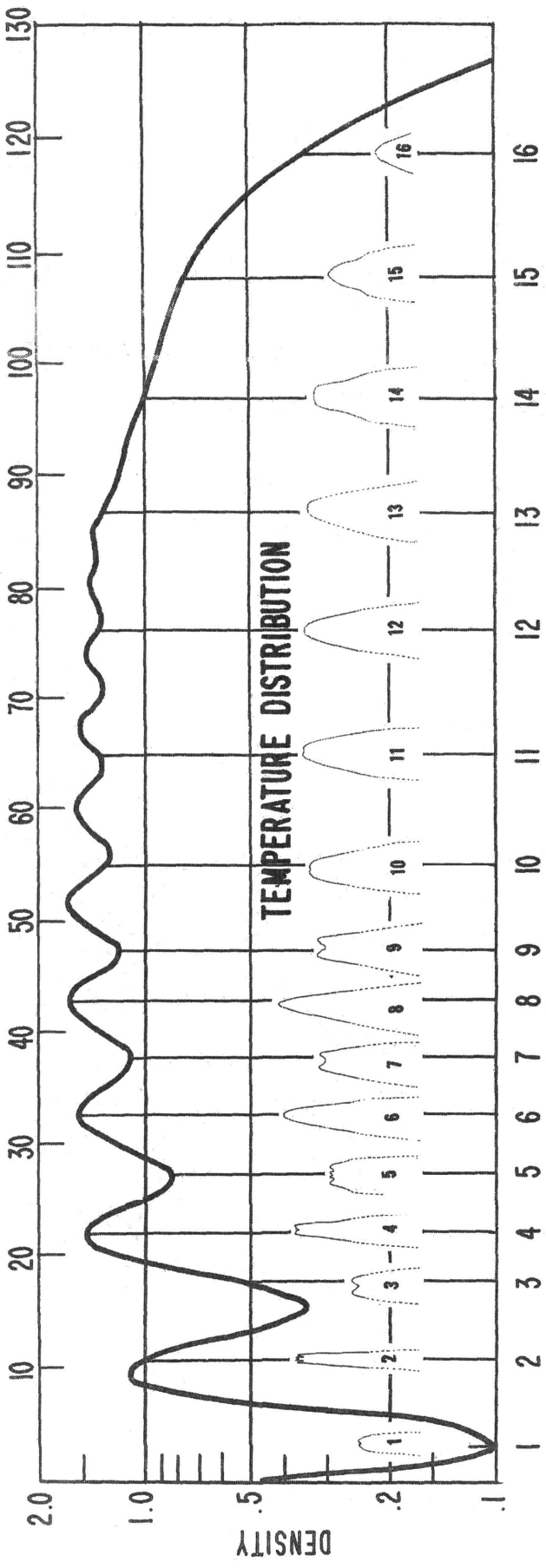


Figure 10 - Motor Run No. 38

This page intentionally left blank.

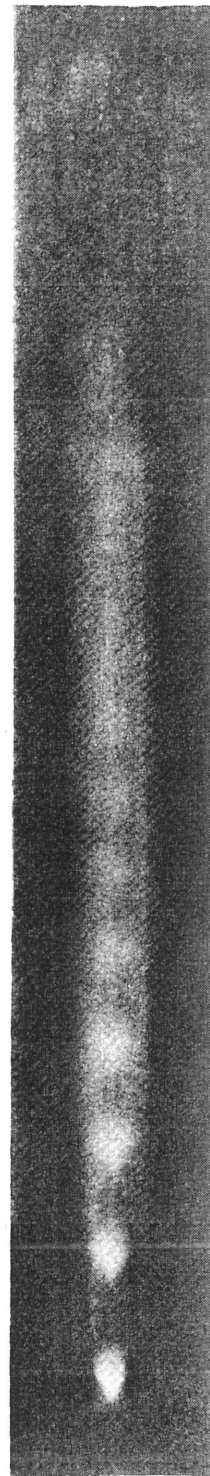
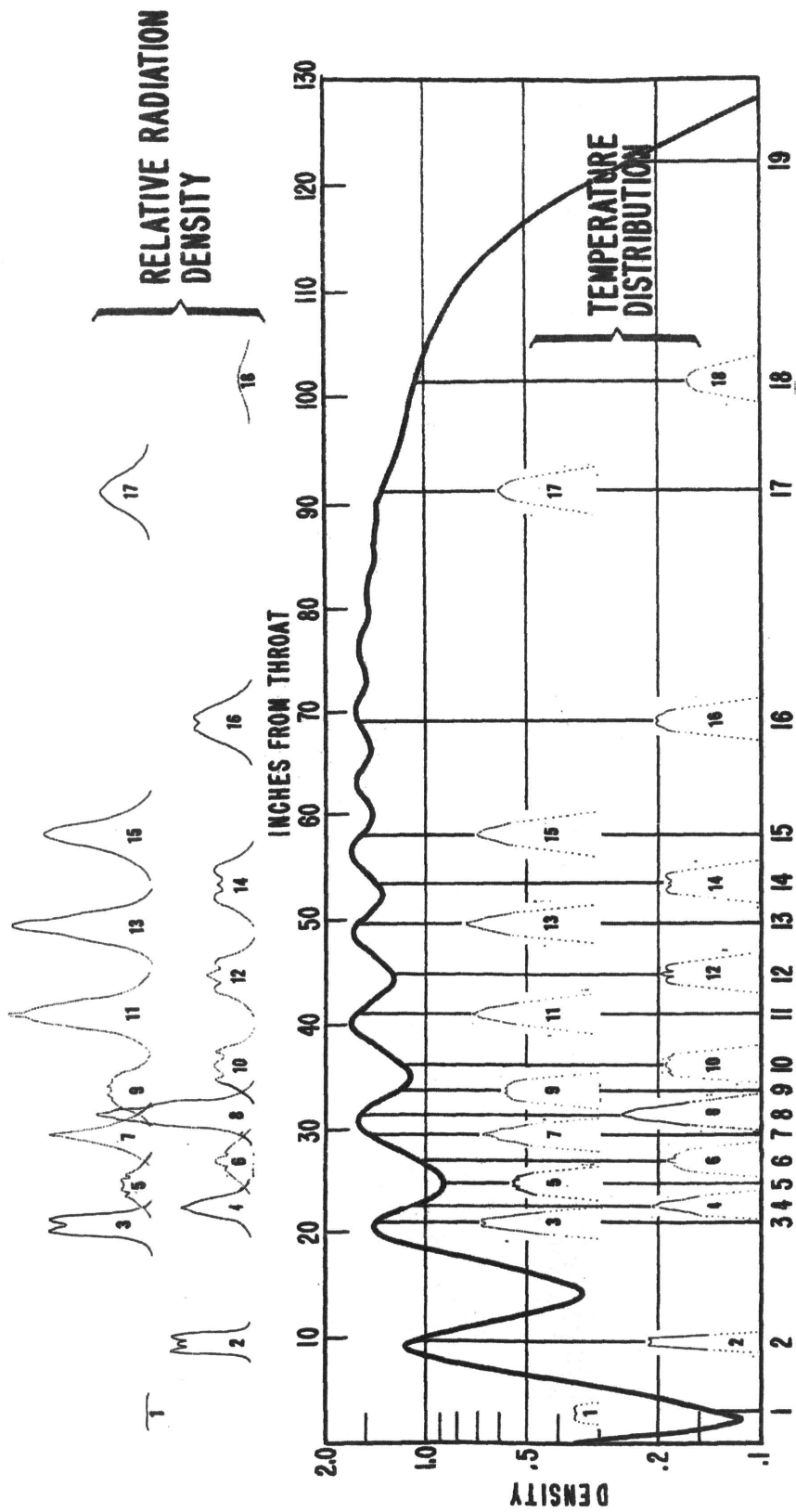


Figure 11 - Motor Run No. 39

This page intentionally left blank.

temperature on the temperature-distribution curves. The general character of the distribution should be essentially correct, and thus an over-all view of the situation can be gained.

The general appearance of the temperature-distribution curves is similar to the corresponding relative-radiation curves, with the exception of a vertical compression of detail at high temperatures due to the logarithmic nature of Equation (6). The points of maximum temperature lie at Mach nodes, the greatest maximum falling at the fourth node in most cases. Since a vast amount of work is required to convert the raw data into radiation density and temperature, only a limited number of points have been presented for each plot (Figures 8, 9, 10, and 11).

In any case, the degree of uncertainty represented by the symmetry assumptions, and that due to graphical differentiation and integration, together do not warrant fine, detailed analysis. In this regard it is noted that the basic theory assumes radial symmetry of the flame. The rocket motors used in this investigation were run near the ground, and thus the cross section is not round. Rather, the edge closest the ground is pulled slightly toward the ground thus, because of Bernoulli's principle, invalidating the assumption requirements slightly. Moreover, the assumptions of known temperature at known points in the flame are open to considerable question. The figure of 2700°K for the acid-aniline motor was taken from actual measurement but upon a different motor and at the center of an unspecified Mach node. The figure of 2600°K for the oxygen-alcohol motor was taken from an actual measurement of a General Electric oxygen-alcohol rocket motor of comparable size. In interpreting the absolute temperature data, all remarks should be prefaced by "If the temperature at a given point is indeed thus, then the distribution is as shown."

SUMMARY

The work with which this report is concerned has resulted in several accomplishments. A satisfactory method for calculating relative radiation density and relative temperature distribution has been developed. A method has been devised for calculating absolute temperature distribution from relative temperature distribution, based upon the assumption that the absolute temperature is known at one point. Although the physical dimensions of the flame and the position of the Mach nodes are presented, caution should be exercised in making use of the results because the photographic method can be in error if rapid oscillation is present in the flame. The plots of relative radiation density and temperature distribution are believed to show correct trends, but graphical differentiation and integration are questionable processes when used to show fine detail.

There results one definite contribution to flame study, namely, the observation that a rocket motor operating in static thrust condition is anything but a uniform, homogeneous barrier to electromagnetic radiation.

FUTURE PLANS

Work of this general nature is continuing in the direction of measurement of flame temperature and particle velocity.

ACKNOWLEDGMENT

The author wishes to acknowledge the assistance of Mr. B. N. Navid in preparing the mathematical section of this report and of Miss E. M. Smith in analyzing the raw data.

* * *